REGULATION OF THE DISTAL TIP COMPLEX CONTROLS CENTRIOLE LENGTH

by

Melanie Zibrat

A Thesis Submitted to the Faculty of the

DEPARTMENT OF CELLULAR AND MOLECULAR MEDICINE

In Partial Fulfillment of the Requirements

For the Degree of

MASTER OF SCIENCE

In the Graduate College

THE UNIVERSITY OF ARIZONA

2019

THE UNIVERSITY OF ARIZONA
GRADUATE COLLEGE

As members of the Master's Committee, we certify that we have read the thesis prepared by Melanie Zibrat, titled Regulation of the Distal Tip Complex Controls Centriole Length and recommend that it be accepted as fulfilling the dissertation requirement for the Master's Degree.

Gregory Rogers, PhD — Date: 5-1-19

Jean Wilson, PhD — Date: 5-1-19

Ghassan Mouneimne, PhD — Date: 05/01/19

Final approval and acceptance of this thesis is contingent upon the candidate's submission of the final copies of the thesis to the Graduate College.

I hereby certify that I have read this thesis prepared under my direction and recommend that it be accepted as fulfilling the Master's requirement.

Gregory Rogers, PhD — Date: 5-1-19
Master's Thesis Committee Chair
Department of Cellular and Molecular Medicine

Acknowledgments

I would like to acknowledge my committee members, Dr. Gregory Rogers, Dr. Jean Wilson, and Dr. Ghassan Mouneimne, for their time and guidance. I would also like to thank past and present members of the Rogers Lab who provided support and/or laughter to my time in the lab: John Ryniawec, Cody Boese, Dr. Daniel Buster, Dr. Tiffany McLamarrah, Dr. Mengdie Wang, Bethany Guice, Sophia Aguirre, Sojal Mahajan, and Hayden Brown.

Table of Contents

Abstract ……...……5

Introduction

Cancer and Genomic Instability …….……..6

Centrosome Amplification and Chromosomal Instability …….…….9

Centriole Structure and Biogenesis ……...….10

Regulation of Centriole Length by the Distal Tip Complex……..……16

Results

Cep97 stabilizes a modified population of CP110…….18

Cep97 stabilizes phosphorylated CP110……..…..20

Carboxy terminal fragment of Cep97 imparts binding and stabilization of CP110……...……21

Cep97 binding promotes phosphorylation of CP110……...……..23

Discussion……...……..24

Materials and Methods…….…...……25

Appendix……...……28

References ……...….30

Abstract

Cancer is one of the most prevalent and deadly diseases worldwide despite the development of an abundance of therapies in the last several decades. Recently, focus has turned to cancer prevention to help mitigate the morbidity of the disease and thus identification of mechanisms that initiate tumorigenesis is of utmost importance. Chromosomal instability is known to be a driver of tumorigenesis and creates vast diversity within the same tumor, allowing for selection and clonal expansion of cells with oncogenic karyotypes. Centrosome amplification is one of the main mechanisms that induces chromosomal instability and does so by creating aberrant attachments to chromosomes during mitosis which often leads to chromosome missegregation. Recent work has identified centriole elongation as a cause of centriole amplification through fragmentation and ectopic procentriole formation, however, how centrioles regulate their length is poorly understood. One proposed method involves antagonistic interactions between CP110, Cep97 and Klp10A at the distal end of centrioles (referred to as the Distal Tip Complex). Previous work in Drosophila has suggested that CP110 limits the centriolar microtubule depolymerizing activity of Klp10A, preventing over-shortening and maintaining the centriole at the correct length. However, how it does so mechanistically is unknown. Even less is known about the activity of centriolar protein Cep97 although previous work proposed it might have a stabilizing role on CP110. Using Drosophila Schneider 2 cells, we investigated the interaction of Cep97 and CP110. Our results suggest that Cep97, through a region in its C-terminal domain, binds and promotes the phosphorylation of CP110, bestowing stabilization.

Introduction

Cancer and Genomic Instability

Cancer is a disease that affects about one in five people worldwide, and accounts for one out of every six deaths (Bray et al., 2018). It is second only to heart disease as a leading cause of mortality and although it is largely a disease of aging, it is also the number one noncommunicable cause of death in children (Siegel et al., 2018). The term "cancer" itself is broad, encompassing over one-hundred different diseases. There is immense variation between and among cancers of different types and thus each case should be treated individually (Fisher et al., 2013). However, identifying universal themes is important for early detection with the aim of preventing disease progression.

Although cancer is a heterogenous group of diseases, all malignant neoplasms require acquisition of several specific phenotypic traits. These so-called "hallmarks" include mechanisms that increase autonomous survival, proliferation, tissue invasion, and evasion of cell death (Hanahan and Weinberg, 2011). Development of these characteristics through mutation is often thought of as a multi-step evolutionary process in which cells gradually accumulate single mutations that convey a growth or survival advantage allowing them to expand clonally and outcompete neighboring cells. However, the normal DNA mutation rate cannot completely explain the complex genome alterations observed in most cancer cells (Greaves and Maley, 2012). The diverse genomes of these cells are instead explained by genomic instability, a state in which cells have an increased rate of accumulating genetic mutations (Giam and Rancati, 2015). Genomic instability can be at both the nucleotide level (nucleotide instability) and chromosomal level (chromosomal instability), although nucleotide instability is mostly dependent on mutations in DNA repair genes and is less frequently seen (Garraway and Lander, 2013). Chromosomal

instability (CIN) results in large-scale alterations such as whole or partial chromosomal deletions, amplifications, inversions, and translocations and thus, excessive CIN is often lethal. However, it is thought that there is a certain tolerance of malignant cells for CIN and at an optimal level it promotes tumor progression through the accumulation of many mutations all at once (Andor et al., 2017). This is supported by the finding that aneuploidy, one of the consequences of CIN, is found in about eighty percent of cancer cells (Knouse et al., 2017).

Although it has been over a hundred years since aneuploidy, the cell state of having an abnormal number of chromosomes, has been proposed as a driver of tumorigenesis, only recently has there been direct evidence for its causal role. In 2007, Weaver et al. published a study in which they used mice heterozygous for a CENP-E null mutation (CENP-$E^{+/-}$) to induce aneuploidy. CENP-E (centromere-associated protein-E) is a kinesin motor protein that is only active during mitosis and functions to maintain the interaction between chromosomes and the mitotic spindle. Due to its absence in interphase, reduced levels of CENP-E have shown to induce aneuploidy without any apparent confounding effects. After about 20 months, CENP-$E^{+/-}$ mice developed significantly more tumors (lymphomas and pulmonary adenomas) than control mice, indicating that aneuploidy is indeed a driver of tumorigenesis. Interestingly, they also found that aneuploidy acts to inhibit tumorigenesis in some cases (Weaver et al., 2007). One possible explanation to this could be that not all CIN-induced karyotypes produce oncogenic phenotypes. Knouse et al. (2017) came to this conclusion after analyzing cancer genome sequencing data from the Cancer Genome Atlas. After identifying several patterns of whole chromosomal gains or losses between and among cancer types, they speculated that under selective pressure, cells that have lost chromosomes carrying combinations with anti-tumorigenic effects and/or have gained chromosomes with genes that in general favor tumorigenesis will outcompete their neighboring cells and initiate tumor

development. Cells that are not so lucky and do not gain advantageous karyotypes are either weeded out by apoptosis or fail to compete with adjacent cells and are not perpetuated (Knouse et al., 2017).

One of the main mechanisms implicated in promoting CIN is chromosome missegregation during mitosis (Giam and Rancati, 2015). For cells to divide into two viable daughter cells, bipolar spindle formation is vital to properly segregate the duplicated genome into each respective cell (Ganem et al., 2009). However, even with the formation of a bipolar spindle there can be errors that occur that disrupt proper segregation of sister chromatids. Normally, the spindle assembly checkpoint (SAC) ensures this proper segregation by detecting and promoting the correction of aberrant spindle attachments. In amphitelic (proper) attachments, those in which sister chromatids are attached to opposite spindle poles, the correct tension is applied to each chromatid and the SAC is satisfied allowing for anaphase onset (Lampson and Cheeseman, 2011). Monotelic and syntelic attachments are improper attachments detected by the SAC in which either only one chromatid is attached to the spindle microtubules (MTs) or when each chromatid is attached by MTs stemming from a single spindle pole, respectively. A single sister chromatid could also be attached by both poles of the spindle in what is called a merotelic attachment. This type of improper attachment is less likely to be detected by the SAC due to proper tension of each chromatid and is therefore a common cause of chromosome missegregation (Musacchio and Salmon, 2007). Centrosome amplification is one mechanism thought to increase the frequency of merotelic attachments and is thus an instigator of CIN (Ganem et al., 2009; Silkworth et al., 2009).

Centrosome Amplification and Chromosomal Instability

Centrosomes are cytoplasmic organelles that function as the microtubule organizing centers (MTOCs) of most animal cells, nucleating and organizing the microtubule cytoskeleton. Their composition can be divided into two main components: the pericentriolar material (PCM), a highly ordered protein matrix that confers microtubule nucleating activity, and the centrioles, two tethered, cylindrically shaped structures that recruit the PCM and act as the duplicating agents of the organelle (Bettencourt-Dias and Glover, 2007; Lawo et al., 2012). During mitosis, two centrosomes are important to establish the bipolar spindle and maintain the fidelity of chromosome segregation (Bettencourt-Dias et al., 2005). Cells with more than two centrosomes (i.e. centrosome amplification) have been shown to produce multipolar spindles in mitosis in which an increased frequency of merotelic attachments are made. In these cases, cells undergo centrosome clustering to produce a pseudo-bipolar spindle prior to anaphase

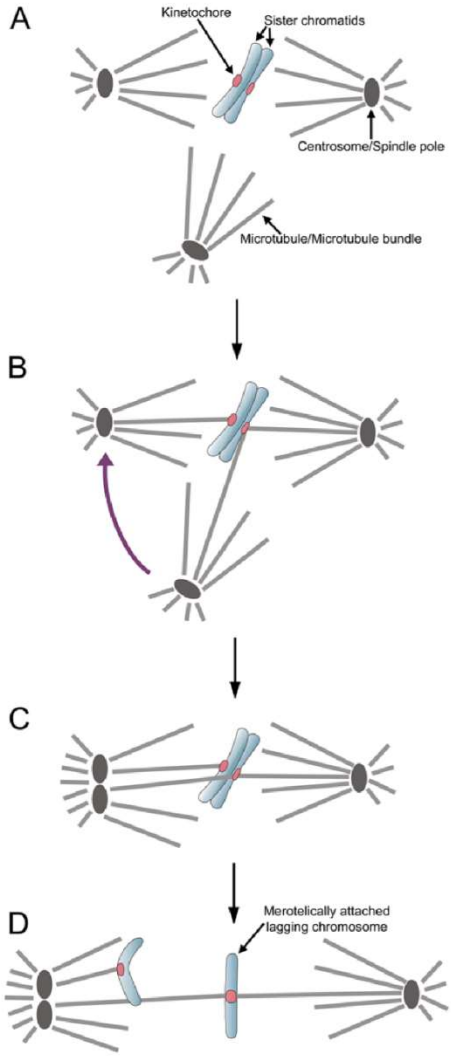

Figure 1. Schematic representation of the mechanism by which multipolarity can lead to merotelic kinetochore attachment and mitotic chromosome mis-segregation. A. Within a multipolar spindle, a single kinetochore is more likely to face two spindle poles than it would be in a bipolar spindle. B. Because of the multipolar spindle geometry, a single kinetochore can easily bind microtubules emanating from two spindle poles rather than from just one pole. After establishment of merotelic kinetochore attachment, the mitotic spindle bi-polarizes by a process of spindle pole coalescence (or centrosome clustering). C. Merotelic kinetochore attachment can persist through metaphase and into anaphase. D. During anaphase, the merotelic kinetochore attachment can give rise to a lagging chromosome. From Silkworth, W.T., I.K. Nardi, L.M. Scholl, and D. Cimini. 2009. Multipolar spindle pole coalescence is a major source of kinetochore mis-attachment and chromosome mis-segregation in cancer cells. PLoS One. 4:e6564. Creative Commons License: http://creativecommons.org/licenses/by/4.0/

onset (Figure 1)(Quintyne et al., 2005). Although this often results in viable cells, the merotelic attachments established earlier in mitosis are frequently left uncorrected and can lead to missegregation of lagging chromosomes (Ganem et al., 2009; Silkworth et al., 2009). To challenge this in vivo, Levine et al. (2017) used transgenic mouse models with inducible expression of Plk4, a kinase important in centriole duplication and, when overexpressed, leads to centrosome amplification. They showed that induction of Plk4 overexpression lead to spontaneous tumor development in the form of lymphomas, squamous cell carcinomas, and sarcomas, indicating a causal role for centrosome amplification in tumorigenesis. Importantly, they showed that both chronic and transient Plk4 overexpression lead to tumor formation, isolating the role of centrosome amplification from indirect effects of constitutive Plk4 activity. This and several other organoid and animal models support the causal role of centrosome amplification in tumor initiation (Basto et al., 2008; Duensing et al., 2001a; Duensing et al., 2001b; Godinho et al., 2014; Goepfert et al., 2002; Shono et al., 2001). Because centrosome amplification seems to be an early event in the progression of many cancers, it is crucial to elucidate the molecular mechanisms in order to gain a better understanding of the disease as a whole and to develop effective therapies (Godinho and Pellman, 2014). A closer look into the structure and biogenesis of centrioles (and the dysregulation thereof) is necessary to provide key insights into the process of centrosome amplification.

Centriole Structure and Biogenesis

As mentioned earlier, centrioles are cylindrical structures that make up centrosomes, however, they are not exclusively a centrosomal constituent. They also make up the basal body of cilia and flagella, two microtubule-composed cellular appendages important in a variety of vital cell functions such as motility, cell signaling, and sensory perception (Bettencourt-Dias and Glover, 2007). Centrioles are made up of stable, modified microtubules, arranged in a nine-fold

radial symmetry that is imparted by a structure called the cartwheel. Stacks of nine rod-shaped Sas6 protein homodimers radiating from their N-terminal contacts, form the "hub" and "spokes" of one tier of often a many-layered cartwheel (van Breugel et al., 2011). Although their size and structure can vary between species and tissues within a species, centriole morphology is relatively well-conserved. *Chlamydomonas reinhardtii* (green algae)*, Drosophila melanogaster* (fruit flies)*, Caenorhabditis elegans* (roundworms), and human cell lines are the four principal centriole model systems due to their many commonalities in regulation and structure (Figure 2)(Kitagawa and Gupta, 2018). Some of the main structural differences between the centrioles in these organisms are the length of the cartwheel (absent in human mother centrioles), the length the microtubules grow past the distal end of the cartwheel (flush with the cartwheel in somatic Drosophila cells), and the number of microtubule sets attached to the cartwheel spokes. The regulatory mechanisms that control these discrepancies is still under investigation, but much has been revealed in the past several decades.

The biogenesis of centrioles can be accomplished by semi-conservative duplication of pre-existing centrioles, by deuterosome formation, or by de novo assembly. The former is the canonical method and the one in which will be described hereafter, while the others occur in multiciliated cells or in the absence of a pre-existing centriole, respectively (Gönczy and Hatzopoulos, 2019). Centriole duplication in this way produces three distinct generations of centrioles: a grandmother, mother, and daughter. A nascent centriole growing off its mother is termed the "procentriole" but becomes the "daughter" when fully mature. In the next cycle, these centrioles are both used for duplication and are thus both "mothers". The older of the two is often referred to as the "grandmother" although its function is the same as the other mother, however distinction may be important in the context of disease (Yamashita et al., 2007).

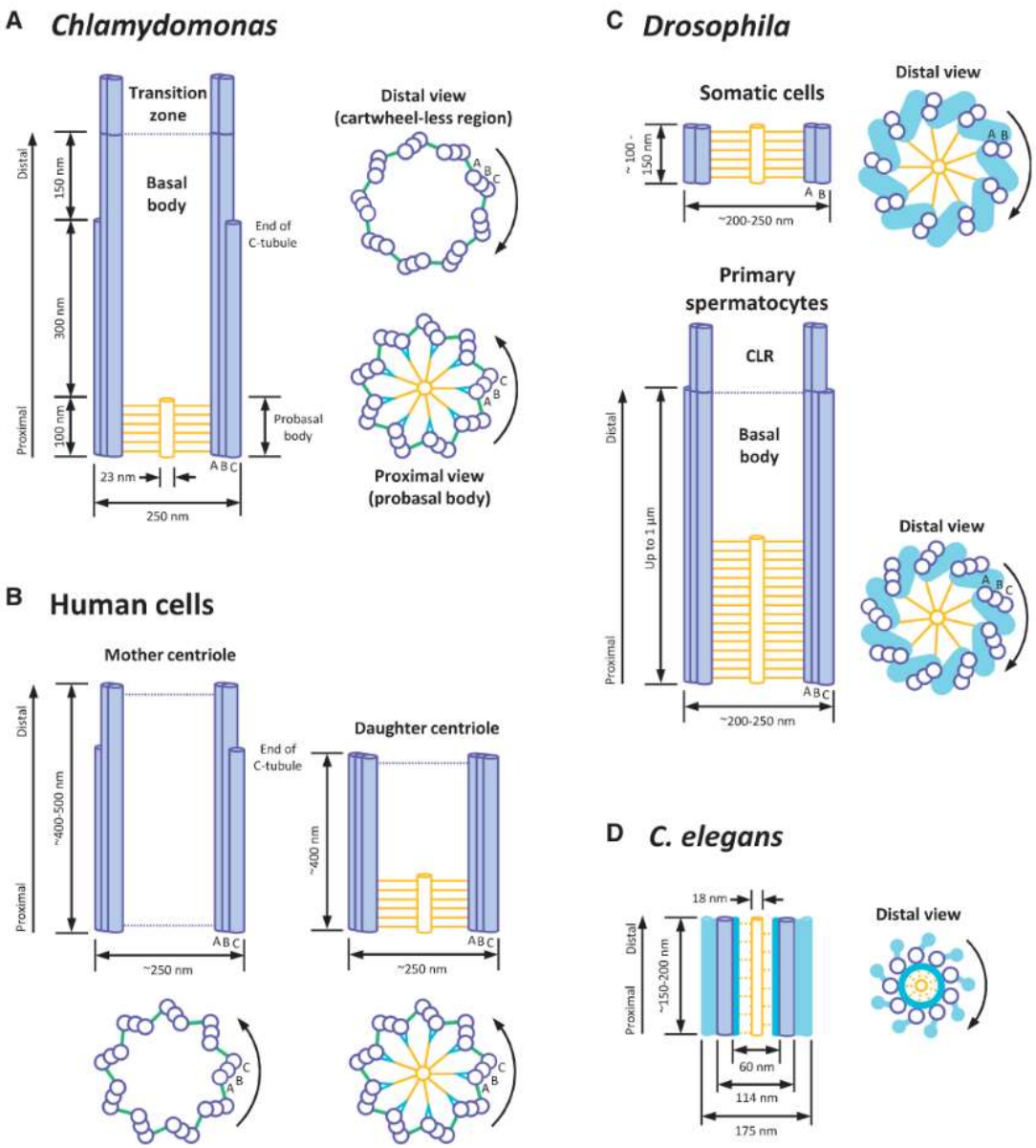

Figure 2. A comparison of centriole structures across common model organisms. Schematic illustrations of centrioles and basal bodies of (A) Chlamydomonas, (B) human cells, (C) Drosophila, and (D) C. elegans. (A, B) Cartwheels are depicted in yellow, centriolar microtubules in purple, the pinhead connecting the cartwheel to the microtubules in blue and the A–C linker in green. Distal and subdistal appendages are not shown in this representation. A-, B-, and C-tubules are indicated on the longitudinal and cross-sections of the centrioles. Note that centriolar microtubules exhibit an anticlockwise twist as seen from the proximal end, and a clockwise twist as seen from the distal end, indicated by the directionality of the curved arrows. (C) Drosophila centrioles consist of several cartwheel stacks (yellow) surrounded by doublet microtubules in somatic cells (top, purple) or triplet microtubules in primary spermatocytes (bottom, purple). Electron–dense structures surrounding the cartwheel are indicated in light blue. CLR, cilium-like region. (D) C. elegans centrioles exhibit a smaller inner tube (yellow) concentric with a central tube (blue). Singlet microtubules (purple) are organized around the central tube, and electron–dense protrusions termed 'paddles' extend from each microtubule (light blue). The possible arrangement of cartwheel spokes is indicated as yellow dotted lines. All dimensions indicated are taken from published sources and the centrioles are depicted on the same scale to the extent possible. From Kitagawa, D., and A. Gupta. 2018. Ultrastructural diversity between centrioles of eukaryotes. The Journal of Biochemistry. 164:1-8, by permission of Oxford University Press.

Centriole duplication is regulated by the cell cycle, one of its many similarities to DNA replication. Before centrioles can duplicate, they must first be "licensed" to do so. One part of licensing is the disengagement of centriole pairs from their tight configuration, mediated by separase and polo-like kinase 1 (PLK1). Separase is a well-known protease involved in the separation of sister chromatids during anaphase by cleavage of cohesion subunits, however, its activity is not as well-understood in centriole disengagement (Gönczy and Hatzopoulos, 2019). This disengagement is necessary for the formation of a procentriole but not sufficient for granting licensure. In humans, proteins Cep152 (Asterless in *Drosophila*), Cep57, and Cep63 form an isotropic complex around the mother centriole, which recruits Plk4 (Lukinavicius et al., 2013). Transient Plk4 activity, stabilized by SCL-interrupting locus protein (STIL) from ubiquitin-mediated degradation, coordinates the single spot in which the procentriole will grow, limiting this event both to once per centriole and per cell cycle (Moyer et al., 2015; Rogers et al., 2009). The details of how this occurs is yet another ongoing area of research and will not be reviewed here. At the end of anaphase, Sas6 is recruited to the proximal centriole by STIL (Ana2 in *Drosophila*) to form the cartwheel, as described previously (Dzhindzhev et al., 2014). Visualization of live *Drosophila* embryos by structured illumination microscopy (SIM) revealed that Sas6 incorporates at the proximal end of the growing cartwheel. In the same study, Plk4 was shown to regulate both the rate and period of centriole growth, suggesting that it may control cartwheel length through Sas6 incorporation (Aydogan et al., 2018). Although Sas6 can self-assemble into cartwheel-like structures in vitro, the fidelity of proper cartwheel assembly is increased with other centriole proteins such as Cep135 (Bld10 in *Chlamydomonas*). This protein localizes to the C-terminus of Sas6 homodimers in an electron dense region known as the pinhead (in humans) that is involved in anchoring microtubules to the cartwheel (Kraatz et al., 2016). Procentrioles begin to elongate in

S phase until they reach a certain length in late mitosis or early G1 (Nigg, 2007). How cells establish and regulate distinct centriole lengths is unclear, however there are several centriole-related proteins that seem to be involved. Elucidation of mechanisms that govern centriole length is imperative as over-elongation of centrioles has been associated with tumorigenesis.

Data from a recent study by Marteil et al. (2018) suggests that over-elongation of centrioles is a cause of chromosome segregation defects by inducing centriole amplification. This group looked at centriole numbers and length in the NCI-60 Human Tumor Cell Lines, a panel of cancer cell lines representative of clinically relevant human cancers from nine different tissues. In these cell lines they found significant increases in centriole number, centriole length, and heterogeneity of centriole length compared to non-transformed lines. After thoroughly validating their methods, they found that more than half of the cancer cell lines had significant centriole amplification (more than 4 centrioles in mitotic cells) compared to the control lines. Importantly, they found that centriole amplification was present in at least one cell line of each tissue type indicating that this phenomenon is not specific to certain tissues but is instead a widespread occurrence in tumors. Overly long centrioles were also found to be common in the NCI-60 panel and, notably, were associated with cell lines containing significant centrosome amplification. To test if overly long centrioles induced centrosome amplification, they overexpressed CPAP in cell lines with normal centriole numbers and lengths. It has been well established that overexpression of CPAP, without obvious indirect effects on centriole duplication, promotes centriole elongation—as was also found in this case (Kohlmaier et al., 2009). A significant percentage of mitotic cells had greater than four centrioles, indicating that over-elongation causes centriole amplification in these cell lines, corroborating findings from previous studies (Kohlmaier et al., 2009; Lin et al., 2013). As concurrent Plk4 overexpression did not suppress amplification in this setting, centriole

fragmentation was suspected. With transmission electron microscopy (TEM) and structured illumination microscopy (SIM) they were able to visualize fragments lacking STIL, indicating these were not newly formed procentrioles. This observation is not novel as fragment-like structures induced by overly long centrioles have been seen previously in both CPAP overexpression and, in *Drosophila,* inhibition of MT depolymerizing Kinesin-13, Klp10a (Delgehyr et al., 2012; Kohlmaier et al., 2009). However, Marteil and colleagues confirmed that these structures were in fact fragments (not procentrioles) not only in CPAP induced centriole elongation, but also found in the NCI-60 cell lines with centrosome amplification. On the other hand, this group also found cases in which STIL-positive centrioles were aberrantly attached along the length of an overly long centriole, suggesting that centriole amplification can also occur by ectopic procentriole formation. As it has been previously suggested that centriole length controls centrosome size and even microtubule nucleating capacity, this group looked at overly long centrioles using NCI-60 cell lines without amplification. Their data indicated that increased centriole length does recruit more PCM and, as a consequence, has stronger microtubule nucleating capacity leading to increased chromosome segregation defects (Marteil et al., 2018). Overall, the findings from this study implicate three mechanisms of chromosomal instability by centriole over-elongation: increased MT nucleating capacity, centrosome amplification by centriole fragmentation, and amplification by ectopic procentriole formation (Figure 3) which altogether underscore the importance of resolving mechanisms that govern centriole length. Interactions between centrosomal proteins Cep97, CP110 and Klp10A at the distal end of centrioles have been proposed as one such mechanism.

Regulation of Centriole Length by the Distal Tip Complex

Evolutionarily conserved and vital for procentriole formation, CP110 localizes to the distal end of both mother and daughter centrioles in cycling cells where it forms a cap-like structure (Chen et al., 2002; Kleylein-Sohn et al., 2007). It has been suggested to have several functions in centriole biogenesis, yet its role as a suppressor of ciliogenesis is the prevailing topic of study. Removal of CP110 from the distal tip is required prior to ciliogenesis and thus its regulation has implications in many ciliopathies (Nigg and Raff, 2009). Surprisingly neglected in the literature,

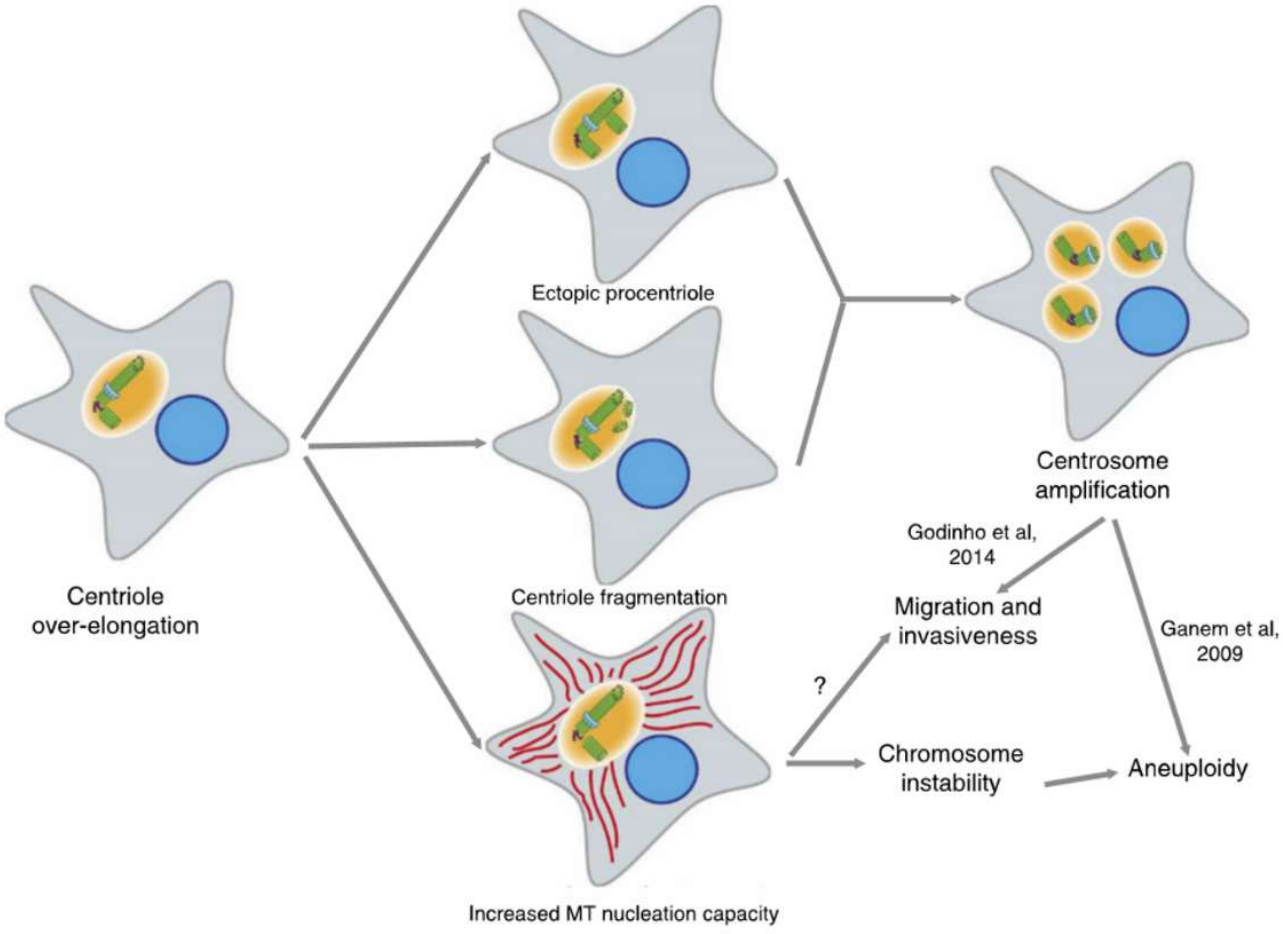

Figure 3. Cellular consequences of centriole length deregulation. In cancer cells, over elongated centrioles induce centriole amplification through centriole fragmentation and/or ectopic procentriole formation along the elongated centrioles. Elongated centrioles also generate larger MTOCs with a higher capacity to nucleate MTs that enhance chromosome instability during mitosis. Both scenarios could give rise to aneuploidy and might as well induce invasiveness, therefore centriole length deregulation might participate to tumour initiation and progression. From Marteil et al., 2018. Over-elongation of centrioles in cancer promotes centriole amplification and chromosome missegregation. Nature communications. 9:1258-1258. Under Creative Commons License: http://creativecommons.org/licenses/by/4.0/

however, is its role in centriole length regulation. This oversight might be explained by the abundance/importance of cilia in mammalian tissues but in *Drosophila* and other centriole-containing organisms where cilia aren't as common, the other roles of CP110 are more apparent. Centrioles elongate through incorporation of αβ-tubulin heterodimers between the distal ends of their nine sets of growing microtubules and the CP110 cap, suggesting that CP110 might play some regulatory role (Kleylein-Sohn et al., 2007). Although depletion of CP110 in cycling human cells leads to overly long centrioles, it has been observed to cause decrease in centriole length in *Drosophila* (Delgehyr et al., 2012; Schmidt et al., 2009). The explanation for this discrepancy is unknown, however may be attributed to the increased complexity of the human system. Klp10A, a kinesin-13 that depolymerizes centriolar MTs, physically interacts with CP110 at the distal tip in *Drosophila*. Delgehyr et al. (2012) investigated this interaction and found that CP110 and Klp10A have antagonistic roles to regulate centriole length. While CP110 depletion makes centrioles shorter, Klp10A depletion leads to centriole elongation and fragmentation. CP110 and Klp10A codepletion results in overly long centrioles, suggesting that CP110 regulates centriole length by limiting the depolymerizing activity of Klp10A. Inhibition of Klp10A activity leads to over elongation of centrioles with or without the presence of CP110, suggesting that although CP110 and Klp10A do physically interact, this interaction is not required for Klp10A recruitment or Klp10A-mediated MT depolymerization (Delgehyr et al., 2012). Instead, Klp10A is thought to localize to centrioles independently due to previously established kinesin-13 microtubule binding ability (Tan et al., 2006). In contrast, CP110 activity and recruitment to the centriole is dependent on another protein: Cep97.

In 2007, Spektor et al. used immunoaffinity purification and subsequent mass spectrometry data in human cell lines to identify CP110 binding partners and found Cep97, a previously

unidentified centrosome-specific protein. Using RNA interference (RNAi) they found that the Cep97-CP110 interaction is crucial for localization of both proteins to the centrosome. Depletion of Cep97 led to not only CP110 disappearance from centrosomes, but overall reduction of CP110 protein levels, while depletion of CP110 did not largely influence total Cep97 levels in the cell. This indicates that Cep97 might act to stabilize CP110. Knockdown of both proteins individually produced the same phenotypes: increased monopolar and multipolar spindles, cytokinesis defects, and premature ciliogenesis (Spektor et al., 2007). The overall conclusion of this paper was that Cep97 and CP110 suppress a ciliogenesis program, however, using similar methods another group interpreted the long structures produced by Cep97 and/or CP110 knockdown as elongated centrioles (Schmidt et al., 2009). Together Klp10A, Cep97, and CP110 form a complex at the distal tip, henceforth referred to as the Distal Tip Complex (DTC), that is fundamental in regulating centriole length. Many questions remain regarding the details of how the DTC works at the molecular level, especially the role of Cep97. Aside from its collaboration with CP110, not much is known about the activity of this protein. We used *Drosophila* Schneider 2 (S2) cells to investigate the action of Cep97 on CP110 in a simple model without cilia to isolate the effects to centriole elongation.

Results

Cep97 stabilizes a modified population of CP110.

As the DTC is important in centriole length regulation, it is important to investigate how the DTC itself is regulated. Because Cep97 depletion decreases CP110 levels but not vice versa, it is thought that its binding somehow stabilizes CP110. With this in mind, we predicted that overexpression of Cep97 would lead to increased CP110 levels. We generated GFP C-terminally tagged Cep97 and

V5 tagged CP110 constructs, co-transfected them into S2 cells, and made whole cell lysate immunoblots with SDS-PAGE. Compared to expression of just GFP and V5-CP110 as a control, V5-CP110 levels were increased more than twofold when co-expressed with Cep97-GFP (Figure 4). Not only did the quantity increase, but the V5-CP110 band had a noticeable band shift upward, indicating a population of V5-CP110 with slightly higher mass (Figure 4, arrow). To confirm this band shift was real and not simply an artifact of overexpression, we made whole cell lysates to look at endogenous CP110 during Cep97 knockdown and in replacement (Cep97-GFP). Knockdown of Cep97 with RNAi collapsed the band shift seen in the presence of both endogenous and exogenous Cep97, confirming physiologic relevance of this pool of higher-mass CP110 (Figure 5). To confirm Cep97 truly has a stabilizing role, we treated V5-CP110 and either GFP or Cep97-GFP expressing S2 cells with cycloheximide (an inhibitor of protein translation) and lysed cells every two hours for eight hours to observe CP110 levels over time (Figure 6). In the GFP control, V5-CP110 bands exhibited a continuous fading over the eight-hour time course, unlike in Cep97-GFP overexpression where protein levels stayed relatively stable until gradually tapering off

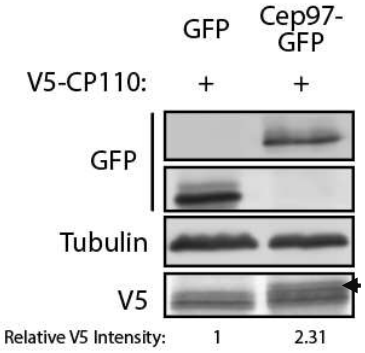

Figure 4. Overexpression of Cep97-GFP both increases V5-CP110 levels twofold and promotes a V5-CP110 bandshift indicating higher molecular weight population of V5-CP110 (arrow). Immunoblots of lysates were made from S2 cells expressing V5-CP110 and either GFP (control) or Cep97-GFP and probed with anti-GFP, -V5, and -tubulin (loading control).

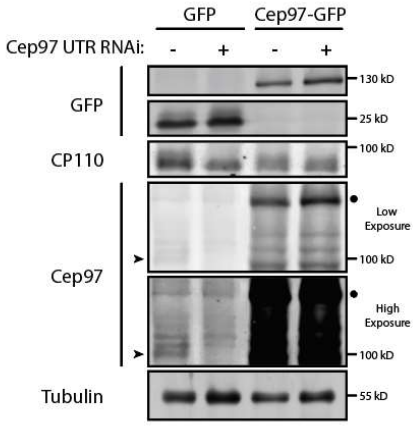

Figure 5. Knockdown of Cep97 collapsed the band shift seen in the presence of both endogenous and exogenous Cep97. Immunoblots of cell lysates were made from S2 cells transfected with or without Cep97 UTR dsRNA (RNAi) and either GFP or Cep97-GFP and stained for anti-GFP, -CP110, -Cep97, and -Tubulin (loading control). Low and high exposure images used to show both endogenous Cep97 (arrowheads) and exogenous Cep97-GFP (dots).

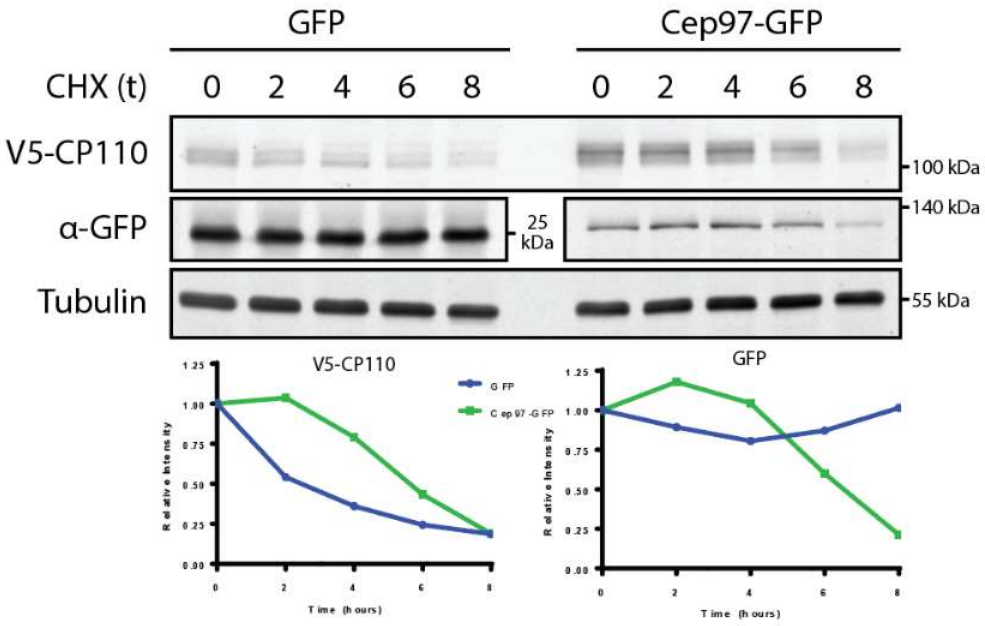

Figure 6. After treatment with cycloheximide, V5-CP110 levels when co-expressed with GFP degraded steadily over eight hours. V5-CP110 when co-expressed with Cep97-GFP stayed relatively constant but began to degrade after four hours somewhat in parallel to the Cep97 signal. S2 cells transfected with V5-CP110 and either GFP or Cep97-GFP were treated with cycloheximide, then lysed at the time points indicated. Cell lysates were used to make western blots and probed with anti-V5, -GFP, -Tubulin (loading control).

after four hours. Interestingly, the degradation seen in the control was especially pronounced in the topmost band whereas in Cep97 overexpression the entirety of V5-CP110 staining faded after eight hours, confirming that Cep97 stabilizes modified CP110. Also of note, Cep97-GFP levels (but not GFP) decreased in similar kinetics to V5-CP110 which could explain the degradation of V5-CP110. Cep97 could possibly be regulated by some unknown mechanism which ultimately controls CP110. Together, these data suggest the presence of Cep97 promotes the stabilization of a post-translationally modified pool of CP110. Our next objective was to determine which post-translational modification was causing the CP110 band shift.

Cep97 stabilizes phosphorylated CP110.

Previous findings established that CP110 is a cyclin E/cyclin-dependent kinase 2 (CDK2) substrate which makes phosphorylation an attractive candidate for the Cep97 promoted CP110

band shift (Chen et al., 2002). To test if it is indeed phosphorylation, we used V5 targeted immunoprecipitation (IP) on S2 cell lysates expressing V5-CP110 and either GFP, Cep97-GFP, or Klp10A-GFP and treated with and without lambda-phosphatase (Figure 7). Consistent with previous findings, without lambda-phosphatase treatment V5-CP110 had a noticeably larger band shift up when co-transfected with Cep97-GFP than with GFP or Klp10A-GFP (Figure 7, arrow). However, lambda-phosphatase treatment collapsed V5-CP110 bands in all conditions into a single lower band, confirming that the modification is in fact phosphorylation. Whether it is Cyclin E/CDK2 phosphorylation is unclear, however, moving forward this will be important to determine.

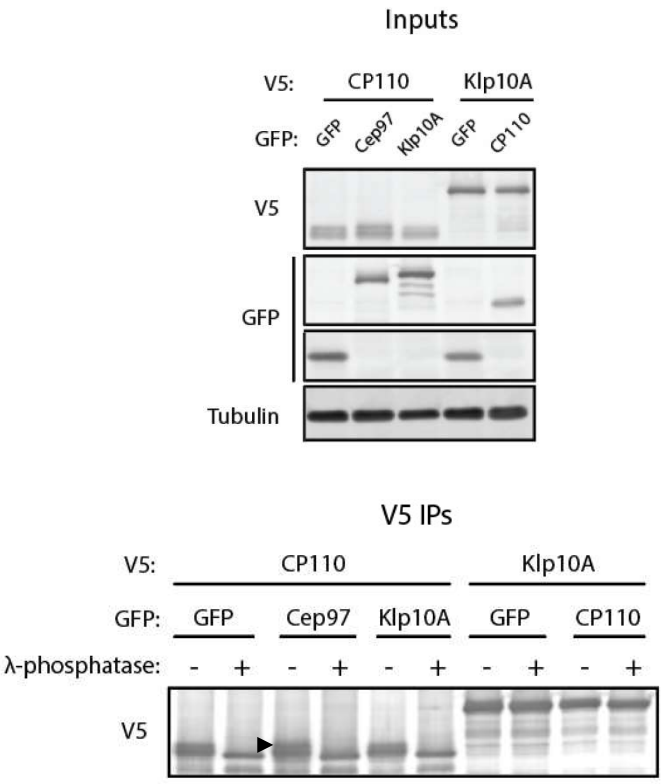

Figure 7. Treatment with lambda-phosphatase collapsed CP110 band shift stabilized by Cep97 (arrowhead).S2 cells were transfected with V5-CP110 and either GFP, Cep97-GFP, or Klp10A-GFP and induced to express 24 hours after. Inputs were created from cell lysates while IP samples were prepared by anti-V5 immunoprecipitation from cell lysates and treated with or without lambda-phosphatase. Immunoblots were probed for GFP, V5, and α-tubulin.

Carboxy-terminal fragment of Cep97 imparts binding and stabilization of CP110.

Previous work identified regions of CP110 (residues 1-223) and Cep97 (residues 300-750) necessary and sufficient for stable Cep97-CP110 binding in humans, however as we are using the *Drosophila* orthologs we identified functional domains within these sequences (Spektor et al., 2007). To identify which region of Cep97 was responsible for binding CP110, we sectioned Cep97

into three distinct fragments: F1 (1-351), F2 (352-513), and F3 (514-806). According to these fragments, we created C-terminally tagged Cep97 truncation mutants with and without each fragment, rendering seven distinct constructs including full-length Cep97 (FL). We co-expressed these constructs with V5-CP110 in S2 cells after RNAi induced knockdown of endogenous Cep97. Co-immunoprecipitation revealed Cep97 fragments containing F3 (FL, ΔF1, ΔF2, F3) were necessary and sufficient to pull down V5-CP110, indicating F3 is responsible for CP110 binding (Figure 8). Also, V5 inputs showed subtle but consistent CP110 band shifts upward only when co-expressed with Cep97 constructs containing F3, indicating that within amino acids 514-806 of Cep97 is a domain that confers stabilization and binding of CP110. Whether these two features of Cep97-F3 are imparted by one or separate entities is unclear, and consequently two competing hypotheses emerge: Cep97 binds a pre-phosphorylated CP110 and blocks degradation or Cep97 binds CP110 and promotes the phosphorylation event leading to stabilization. Finding the phosphorylation site will be an important step moving forward as phosphomimetics could clarify this and other questions regarding the ability this modification bestows.

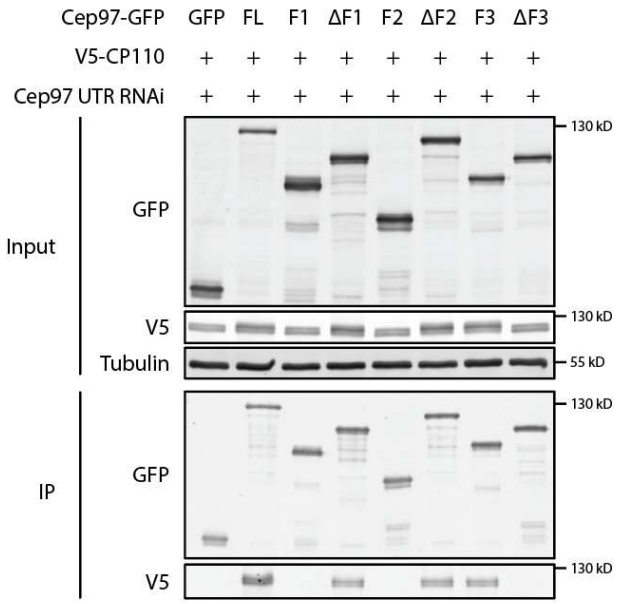

Figure 8. F3 of Cep97 is necessary and sufficient for binding CP110 and stabilizing specific phosphorylated CP110 pool. All and only constructs containing F3 (FL, ΔF1, ΔF2, F3) pulled down V5-CP110 during immunoprecipitation. Cell lysates were created from S2 cells transfected with Cep97 UTR dsRNA, V5-CP110, and either GFP or the various Cep97 constructs. Anti-GFP Immunoprecipitation was used and immunoblots were stained with anti-GFP, -V5, and Tubulin antibodies.

Cep97 binding promotes phosphorylation of CP110.

In humans, CP110 is ubiquitinated and sent for proteasomal degradation by $SCF^{Cyclin\ F}$ and thus we suspected CP110 would be degraded by the proteasome in *Drosophila* as well (D'Angiolella et al., 2010). To test whether Cep97 activity was preventing CP110 from proteasomal degradation, we implemented proteasome inhibitor MG132 (Lee and Goldberg, 1998). We depleted Cep97 using RNAi in S2 cells then treated with MG132 or DMSO for five hours prior to lysing (Figure 9). Immunoblots of cell lysates using antibodies against endogenous CP110 showed reversal of Cep97 knockdown-induced CP110 depletion with MG132 treatment compared to DMSO control, confirming proteasomal degradation of CP110 in *Drosophila*. These results also indicate that Cep97 does prevent CP110 degradation, however, the CP110 band seen after proteasomal inhibition with concurrent Cep97 depletion did not show the typical Cep97-promoted phosphorylation. Compared to CP110 from cells transfected with control RNA (PET28a dsRNA) and treated with DMSO (representing the physiologic CP110 population), CP110 ran as a thinner band in the experimental condition (representing the population of CP110 that would have been degraded without Cep97). This suggests that Cep97 does not bind and stabilize phosphorylated CP110 but instead plays a role in promoting phosphorylation.

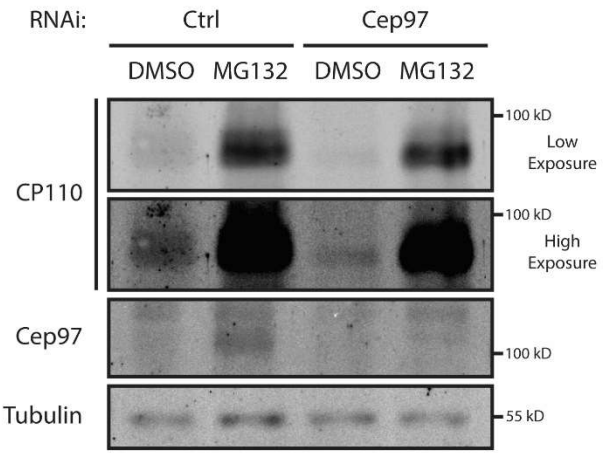

Figure 9. Drosophila CP110 is stabilized by proteasome inhibitor MG132. MG132 rescues Cep97 knockdown induced collapse of CP110 band shift. S2 cells were treated with either Ctrl (PET28a) or Cep97 UTR dsRNA for 6 days. On the 7th day cells were either treated with DMSO (control) or MG132 and incubated for 5 hours prior to lysing. Immunoblots of samples were stained with anti-CP110, -Cep97, and -Tubulin (loading control).

Discussion

Many questions remain about the mechanism of which Cep97 stabilizes CP110, including how Cep97 promotes phosphorylation. To seek the answer of this, finding the kinase responsible will be important. As mentioned earlier, CP110 is a CycE/CDK2 substrate, although it is unknown whether this complex is accountable for all of CP110 phosphorylation (Chen et al., 2002). Further experimentation would be important to identify if CDK2 was responsible for this Cep97 stabilization specific phosphorylation. Another crucial discovery will be the mechanism by which this phosphorylation stabilizes CP110 levels. One possibility could be the phosphorylation-dependent recruitment or binding of a deubiquitinating enzyme (DUB) that removes constitutive ubiquitination. In 2013, Li et al. identified a DUB, USP33, that stabilizes CP110 levels during centriole duplication in human cells. The same has yet to be reported in *Drosophila*, however, there is a protein that shares homology. Identification of both the phosphorylation site and ubiquitin site could yield more insight. CP110 localizes to both the mother and daughter centriole during the cell cycle, but because the mother centriole maintains its length throughout there may be a mechanism involving dissimilar CP110 phosphorylation states at the two sites. It would be of interest to identify the spatial differences of varying phospho-CP110 pools.

In conclusion, our data suggests that Cep97, through fragment three in its C-terminal domain, binds and promotes the phosphorylation and stabilization of CP110. This allows CP110 to localize to the distal tip of the centriole and interact with Klp10A, regulating centriole length. Dysregulation of the interactions of the DTC can lead to centriole elongation, which through fragmentation and procentriole formation can cause centrosome amplification. Understanding the underlying mechanisms of centrosome amplification is crucial as it is known to cause genomic instability, one of the hallmarks of cancer.

Materials and Methods

Drosophila cell culture

Drosophila S2 cell culture was performed as previously described (Rogers and Rogers, 2008). S2 cells (Life Technologies; catalogue no. R69007) were cultured at room temperature (20–25°C) in Sf900II SFM medium (Life Technologies; catalogue no. 10902104).

Double-stranded RNA (dsRNA) interference

dsRNA interference (RNAi) was performed as previously described (Rogers and Rogers, 2008). Briefly, cells were cultured in six-well plates at 50–90% confluency in 1 ml of medium. Cells were treated with 10 µg dsRNA every day for 5-7 d. Control dsRNA was synthesized from noncoding DNA in a pET28a vector template (Clontech) using the primers 5′-ATCAG GCGCTCTTCCGC and 5′-GTTCGTGCACACAGCCC. Generated a Cep97 5'-3' UTR fusion construct by mutagenizing to delete coding region from EST using the following primers: 97Fus-1: CGGCCTGCCAATCAGAAAAACAAATCCCAGTTAATAAATGAGGAGTATAAACGCT TTAAGGGTCG and 97Fus-2: CGACCCTTAAAGCGTTTATACTCCTCATTTATTAACTGG GATTTGTTTTTCTGATTGGCAGGCCG. T7 Template was generated from 5'-3' UTR fusion through PCR amplification using primers: 97UTRT7-F: TAATACGACTCACTATAGGG GTCGAGAGCGGAGACG and 97UTRT7-R: TAATACGACTCACTATAGGG ACTATTGTTAAGTCTTCCACCATCGC.

Immunoblotting

S2 cell lysates were produced by lysing cells in cold PBS containing 0.1% Triton X-100. Laemmli sample buffer was then added and the samples were boiled for 5 min. Samples of equal total protein

were resolved by SDS–PAGE, blotted, probed with primary and secondary antibodies, and scanned on an Odyssey imager (Li-Cor Biosciences). Care was taken to avoid saturating the scans of blots. Antibodies used for Western blotting include chicken anti-Cep97 (our laboratory), guinea pig anti-CP110 (our laboratory), mouse anti-GFP monoclonal JL-8 (Clontech; catalogue no. 632380), mouse anti-V5 monoclonal (Life Technologies; catalogue no. R960-25), and mouse anti-a tubulin (Sigma-Aldrich; catalogue no. T9026) at dilutions ranging from 1:1000 to 1:3000. IRDye 800CW secondary antibodies (Li-Cor Biosciences) were prepared according to manufacturer's instructions and used at dilutions ranging from 1:1500 to 1:3000 dilution.

Constructs and transfection

FL cDNAs of Drosophila CP110, Cep97, Klp10A were subcloned into a pMT vector containing in-frame coding sequences for EGFP or V5 under control of the inducible metallothionein promoter. Mutants of Cep97 were generated by PCR-based site directed mutagenesis with Phusion polymerase (ThermoFisher; catalogue no. F530S). For transient transfections, (2–5) × 10^6 S2 cells were pelleted by centrifugation and resuspended in 100 µl of transfection solution (5 mM KCl, 15 mM MgCl2, 120 mM sodium phosphate, 50 mM d-mannitol, pH 7.2) containing 2 µg of purified plasmid. The resuspension was then transferred to a 2-mm gap cuvette and electroporated using a Nucleofector 2b (Lonza), program G-030. Transfected cells were immediately diluted in 1 ml of SF-900 II medium and placed in a six-well tissue culture plate. Cells were typically allowed to recover for ~24 h before inducing by the addition of 0.5–2 mM CuSO4 to the culture medium. For cycloheximide assay, 100 ug/mL cycloheximide (Sigma) was added to 5 wells of each condition at time 0. A single well of each condition was lysed at 0, 2, 4, 6, and 8 hours. Band intensities were

quantified using ImageJ and normalized to tubulin load, values are compared to normalized intensity at Time 0.

Immunoprecipitation assays

GFP-binding protein (GBP)(Rothbauer et al., 2008) was fused to the Fc domain of human IgG (pIg-Tail; R&D Systems), tagged with His6 in pET28a (EMD Biosciences), expressed in Escherichia coli, and purified on HisPur resin (ThermoFisher; catalogue no. 88221) as described previously (Buster et al., 2013). Purified GBP was bound to magnetic Dyna Beads (ThermoFisher; catalogue no. 10001D), and then cross-linked to the resin by incubating with 20 mM dimethyl pimelimidate dihydrochloride in PBS, pH 8.3, 2 h at 22°C, then quenched by incubation with 0.2 M ethanolamine, pH 8.3, 1 h at 22°C. Antibody-coated beads were washed three times with PBSTween20 (0.02%), then equilibrated in 1.0 ml of cell lysis buffer (CLB; 50 mM Tris, pH 7.2, 125 mM NaCl, 2 mM DTT, 0.1% Triton X-100, and 0.1 mM phenylmethylsulfonyl fluoride [PMSF]). Transfected cells expressing recombinant proteins were lysed in CLB, and the lysates clarified by centrifugation at 16,100 × g for 5 min at 4°C. Inputs (0.5–1%) were used for immunoblots. GBP-coated beads were rocked with lysate for 30 min at 4°C, washed three times with 1 ml CLB, and then boiled in Laemmli sample buffer.

For V5-immunoprecipitation anti-V5 antibodies (Invitrogen) were coupled to Protein G Dynabeads (Invitrogen). IP protocol was as described for GFP. Final IPs were split in half and incubated at 30C for 30 minutes in phosphatase buffer (NEB) + 20 mM MnCl2 with or without lambda phosphatase (housemade), buffer was removed, then IP was eluted as normal.

Appendix

OXFORD UNIVERSITY PRESS LICENSE
TERMS AND CONDITIONS

Apr 16, 2019

This Agreement between Melanie Zibrat ("You") and Oxford University Press ("Oxford University Press") consists of your license details and the terms and conditions provided by Oxford University Press and Copyright Clearance Center.

License Number	4570990887429
License date	Apr 16, 2019
Licensed content publisher	Oxford University Press
Licensed content publication	The Journal of Biochemistry
Licensed content title	Ultrastructural diversity between centrioles of eukaryotes
Licensed content author	Gupta, Akshari; Kitagawa, Daiju
Licensed content date	Feb 16, 2018
Type of Use	Thesis/Dissertation
Institution name	
Title of your work	REGULATION OF THE DISTAL TIP COMPLEX CONTROLS CENTRIOLE LENGTH
Publisher of your work	University of Arizona
Expected publication date	May 2019
Permissions cost	0.00 USD
Value added tax	0.00 USD
Total	0.00 USD
Title	REGULATION OF THE DISTAL TIP COMPLEX CONTROLS CENTRIOLE LENGTH
Institution name	University of Arizona
Expected presentation date	May 2019
Portions	Figure 1
Requestor Location	Melanie Zibrat 
Publisher Tax ID	GB125506730
Total	0.00 USD
Terms and Conditions	

STANDARD TERMS AND CONDITIONS FOR REPRODUCTION OF MATERIAL FROM AN OXFORD UNIVERSITY PRESS JOURNAL

1. Use of the material is restricted to the type of use specified in your order details.
2. This permission covers the use of the material in the English language in the following territory: world. If you have requested additional permission to translate this material, the

terms and conditions of this reuse will be set out in clause 12.
3. This permission is limited to the particular use authorized in (1) above and does not allow you to sanction its use elsewhere in any other format other than specified above, nor does it apply to quotations, images, artistic works etc that have been reproduced from other sources which may be part of the material to be used.
4. No alteration, omission or addition is made to the material without our written consent. Permission must be re-cleared with Oxford University Press if/when you decide to reprint.
5. The following credit line appears wherever the material is used: author, title, journal, year, volume, issue number, pagination, by permission of Oxford University Press or the sponsoring society if the journal is a society journal. Where a journal is being published on behalf of a learned society, the details of that society must be included in the credit line.
6. For the reproduction of a full article from an Oxford University Press journal for whatever purpose, the corresponding author of the material concerned should be informed of the proposed use. Contact details for the corresponding authors of all Oxford University Press journal contact can be found alongside either the abstract or full text of the article concerned, accessible from www.oxfordjournals.org Should there be a problem clearing these rights, please contact journals.permissions@oup.com
7. If the credit line or acknowledgement in our publication indicates that any of the figures, images or photos was reproduced, drawn or modified from an earlier source it will be necessary for you to clear this permission with the original publisher as well. If this permission has not been obtained, please note that this material cannot be included in your publication/photocopies.
8. While you may exercise the rights licensed immediately upon issuance of the license at the end of the licensing process for the transaction, provided that you have disclosed complete and accurate details of your proposed use, no license is finally effective unless and until full payment is received from you (either by Oxford University Press or by Copyright Clearance Center (CCC)) as provided in CCC's Billing and Payment terms and conditions. If full payment is not received on a timely basis, then any license preliminarily granted shall be deemed automatically revoked and shall be void as if never granted. Further, in the event that you breach any of these terms and conditions or any of CCC's Billing and Payment terms and conditions, the license is automatically revoked and shall be void as if never granted. Use of materials as described in a revoked license, as well as any use of the materials beyond the scope of an unrevoked license, may constitute copyright infringement and Oxford University Press reserves the right to take any and all action to protect its copyright in the materials.
9. This license is personal to you and may not be sublicensed, assigned or transferred by you to any other person without Oxford University Press's written permission.
10. Oxford University Press reserves all rights not specifically granted in the combination of (i) the license details provided by you and accepted in the course of this licensing transaction, (ii) these terms and conditions and (iii) CCC's Billing and Payment terms and conditions.
11. You hereby indemnify and agree to hold harmless Oxford University Press and CCC, and their respective officers, directors, employs and agents, from and against any and all claims arising out of your use of the licensed material other than as specifically authorized pursuant to this license.
12. Other Terms and Conditions:
v1.4

Questions? customercare@copyright.com or +1-855-239-3415 (toll free in the US) or +1-978-646-2777.

References

Andor, N., C.C. Maley, and H.P. Ji. 2017. Genomic Instability in Cancer: Teetering on the Limit of Tolerance. *Cancer Res*. 77:2179-2185.

Aydogan, M.G., A. Wainman, S. Saurya, T.L. Steinacker, A. Caballe, Z.A. Novak, J. Baumbach, N. Muschalik, and J.W. Raff. 2018. A homeostatic clock sets daughter centriole size in flies. *The Journal of Cell Biology*. 217:1233.

Basto, R., K. Brunk, T. Vinadogrova, N. Peel, A. Franz, A. Khodjakov, and J.W. Raff. 2008. Centrosome Amplification Can Initiate Tumorigenesis in Flies. *Cell*. 133:1032-1042.

Bettencourt-Dias, M., and D.M. Glover. 2007. Centrosome biogenesis and function: centrosomics brings new understanding. *Nat Rev Mol Cell Biol*. 8:451-463.

Bettencourt-Dias, M., A. Rodrigues-Martins, L. Carpenter, M. Riparbelli, L. Lehmann, M.K. Gatt, N. Carmo, F. Balloux, G. Callaini, and D.M. Glover. 2005. SAK/PLK4 is required for centriole duplication and flagella development. *Curr Biol*. 15:2199-2207.

Bray, F., J. Ferlay, I. Soerjomataram, R.L. Siegel, L.A. Torre, and A. Jemal. 2018. Global cancer statistics 2018: GLOBOCAN estimates of incidence and mortality worldwide for 36 cancers in 185 countries. *CA: A Cancer Journal for Clinicians*. 68:394-424.

Buster, D.W., S.G. Daniel, H.Q. Nguyen, S.L. Windler, L.C. Skwarek, M. Peterson, M. Roberts, J.H. Meserve, T. Hartl, J.E. Klebba, D. Bilder, G. Bosco, and G.C. Rogers. 2013. SCFSlimb ubiquitin ligase suppresses condensin II-mediated nuclear reorganization by degrading Cap-H2. *The Journal of cell biology*. 201:49-63.

Chen, Z., V.B. Indjeian, M. McManus, L. Wang, and B.D. Dynlacht. 2002. CP110, a Cell Cycle-Dependent CDK Substrate, Regulates Centrosome Duplication in Human Cells. *Developmental Cell*. 3:339-350.

Delgehyr, N., H. Rangone, J. Fu, G. Mao, B. Tom, Maria G. Riparbelli, G. Callaini, and David M. Glover. 2012. Klp10A, a Microtubule-Depolymerizing Kinesin-13, Cooperates with CP110 to Control Drosophila Centriole Length. *Current Biology*. 22:502-509.

Duensing, S., A. Duensing, C.P. Crum, and K. Münger. 2001a. Human Papillomavirus Type 16 E7 Oncoprotein-induced Abnormal Centrosome Synthesis Is an Early Event in the Evolving Malignant Phenotype. *Cancer Research*. 61:2356.

Duensing, S., A. Duensing, E.R. Flores, A. Do, P.F. Lambert, and K. Münger. 2001b. Centrosome Abnormalities and Genomic Instability by Episomal Expression of Human Papillomavirus Type 16 in Raft Cultures of Human Keratinocytes. *Journal of Virology*. 75:7712.

Dzhindzhev, Nikola S., G. Tzolovsky, Z. Lipinszki, S. Schneider, R. Lattao, J. Fu, J. Debski, M. Dadlez, and David M. Glover. 2014. Plk4 Phosphorylates Ana2 to Trigger Sas6 Recruitment and Procentriole Formation. *Current Biology*. 24:2526-2532.

D'Angiolella, V., V. Donato, S. Vijayakumar, A. Saraf, L. Florens, M.P. Washburn, B. Dynlacht, and M. Pagano. 2010. SCFCyclin F controls centrosome homeostasis and mitotic fidelity through CP110 degradation. *Nature*. 466:138.

Fisher, R., L. Pusztai, and C. Swanton. 2013. Cancer heterogeneity: implications for targeted therapeutics. *British Journal Of Cancer*. 108:479.

Ganem, N.J., S.A. Godinho, and D. Pellman. 2009. A mechanism linking extra centrosomes to chromosomal instability. *Nature*. 460:278-282.

Garraway, Levi A., and Eric S. Lander. 2013. Lessons from the Cancer Genome. *Cell*. 153:17-37.

Giam, M., and G. Rancati. 2015. Aneuploidy and chromosomal instability in cancer: a jackpot to chaos. *Cell Division*. 10:3.
Godinho, S.A., and D. Pellman. 2014. Causes and consequences of centrosome abnormalities in cancer. *Philosophical Transactions of the Royal Society B: Biological Sciences*. 369:20130467.
Godinho, S.A., R. Picone, M. Burute, R. Dagher, Y. Su, C.T. Leung, K. Polyak, J.S. Brugge, M. Théry, and D. Pellman. 2014. Oncogene-like induction of cellular invasion from centrosome amplification. *Nature*. 510:167-171.
Goepfert, T.M., Y.E. Adigun, L. Zhong, J. Gay, D. Medina, and W.R. Brinkley. 2002. Centrosome Amplification and Overexpression of Aurora A Are Early Events in Rat Mammary Carcinogenesis. *Cancer Research*. 62:4115.
Greaves, M., and C.C. Maley. 2012. Clonal evolution in cancer. *Nature*. 481:306-313.
Gönczy, P., and G.N. Hatzopoulos. 2019. Centriole assembly at a glance. *Journal of Cell Science*. 132:jcs228833.
Hanahan, D., and R.A. Weinberg. 2011. Hallmarks of cancer: the next generation. *Cell*. 144:646-674.
Kitagawa, D., and A. Gupta. 2018. Ultrastructural diversity between centrioles of eukaryotes. *The Journal of Biochemistry*. 164:1-8.
Kleylein-Sohn, J., J. Westendorf, M. Le Clech, R. Habedanck, Y.-D. Stierhof, and E.A. Nigg. 2007. Plk4-Induced Centriole Biogenesis in Human Cells. *Developmental Cell*. 13:190-202.
Knouse, K.A., T. Davoli, S.J. Elledge, and A. Amon. 2017. Aneuploidy in Cancer: Seq-ing Answers to Old Questions. *Annual Review of Cancer Biology*. 1:335-354.
Kohlmaier, G., J. Lončarek, X. Meng, B.F. McEwen, M.M. Mogensen, A. Spektor, B.D. Dynlacht, A. Khodjakov, and P. Gönczy. 2009. Overly Long Centrioles and Defective Cell Division upon Excess of the SAS-4-Related Protein CPAP. *Current Biology*. 19:1012-1018.
Kraatz, S., P. Guichard, Jagan M. Obbineni, N. Olieric, Georgios N. Hatzopoulos, M. Hilbert, I. Sen, J. Missimer, P. Gönczy, and Michel O. Steinmetz. 2016. The Human Centriolar Protein CEP135 Contains a Two-Stranded Coiled-Coil Domain Critical for Microtubule Binding. *Structure*. 24:1358-1371.
Lampson, M.A., and I.M. Cheeseman. 2011. Sensing centromere tension: Aurora B and the regulation of kinetochore function. *Trends in Cell Biology*. 21:133-140.
Lawo, S., M. Hasegan, G.D. Gupta, and L. Pelletier. 2012. Subdiffraction imaging of centrosomes reveals higher-order organizational features of pericentriolar material. *Nature Cell Biology*. 14:1148.
Lee, D.H., and A.L. Goldberg. 1998. Proteasome inhibitors: valuable new tools for cell biologists. *Trends in Cell Biology*. 8:397-403.
Lin, Y.-N., C.-T. Wu, Y.-C. Lin, W.-B. Hsu, C.-J.C. Tang, C.-W. Chang, and T.K. Tang. 2013. CEP120 interacts with CPAP and positively regulates centriole elongation. *The Journal of Cell Biology*. 202:211.
Lukinavicius, G., D. Lavogina, M. Orpinell, K. Umezawa, L. Reymond, N. Garin, P. Gonczy, and K. Johnsson. 2013. Selective chemical crosslinking reveals a Cep57-Cep63-Cep152 centrosomal complex. *Curr Biol*. 23:265-270.
Marteil, G., A. Guerrero, A.F. Vieira, B.P. de Almeida, P. Machado, S. Mendonça, M. Mesquita, B. Villarreal, I. Fonseca, M.E. Francia, K. Dores, N.P. Martins, S.C. Jana, E.M.

Tranfield, N.L. Barbosa-Morais, J. Paredes, D. Pellman, S.A. Godinho, and M. Bettencourt-Dias. 2018. Over-elongation of centrioles in cancer promotes centriole amplification and chromosome missegregation. *Nature communications*. 9:1258-1258.

Moyer, T.C., K.M. Clutario, B.G. Lambrus, V. Daggubati, and A.J. Holland. 2015. Binding of STIL to Plk4 activates kinase activity to promote centriole assembly. *The Journal of Cell Biology*. 209:863.

Musacchio, A., and E.D. Salmon. 2007. The spindle-assembly checkpoint in space and time. *Nature Reviews Molecular Cell Biology*. 8:379.

Nigg, E.A. 2007. Centrosome duplication: of rules and licenses. *Trends in Cell Biology*. 17:215-221.

Nigg, E.A., and J.W. Raff. 2009. Centrioles, Centrosomes, and Cilia in Health and Disease. *Cell*. 139:663-678.

Quintyne, N.J., J.E. Reing, D.R. Hoffelder, S.M. Gollin, and W.S. Saunders. 2005. Spindle Multipolarity Is Prevented by Centrosomal Clustering. *Science*. 307:127.

Rogers, G.C., N.M. Rusan, D.M. Roberts, M. Peifer, and S.L. Rogers. 2009. The SCF^{Slimb} ubiquitin ligase regulates Plk4/Sak levels to block centriole reduplication. *The Journal of Cell Biology*. 184:225.

Rogers, S.L., and G.C. Rogers. 2008. Culture of Drosophila S2 cells and their use for RNAi-mediated loss-of-function studies and immunofluorescence microscopy. *Nature Protocols*. 3:606.

Rothbauer, U., K. Zolghadr, S. Muyldermans, A. Schepers, M.C. Cardoso, and H. Leonhardt. 2008. A Versatile Nanotrap for Biochemical and Functional Studies with Fluorescent Fusion Proteins. *Molecular & Cellular Proteomics*. 7:282.

Schmidt, T.I., J. Kleylein-Sohn, J. Westendorf, M. Le Clech, S.B. Lavoie, Y.-D. Stierhof, and E.A. Nigg. 2009. Control of Centriole Length by CPAP and CP110. *Current Biology*. 19:1005-1011.

Shono, M., N. Sato, K. Mizumoto, N. Maehara, M. Nakamura, E. Nagai, and M. Tanaka. 2001. Stepwise Progression of Centrosome Defects Associated with Local Tumor Growth and Metastatic Process of Human Pancreatic Carcinoma Cells Transplanted Orthotopically into Nude Mice. *Laboratory Investigation*. 81:945.

Siegel, R.L., K.D. Miller, and A. Jemal. 2018. Cancer statistics, 2018. *CA Cancer J Clin*. 68:7-30.

Silkworth, W.T., I.K. Nardi, L.M. Scholl, and D. Cimini. 2009. Multipolar spindle pole coalescence is a major source of kinetochore mis-attachment and chromosome mis-segregation in cancer cells. *PLoS One*. 4:e6564.

Spektor, A., W.Y. Tsang, D. Khoo, and B.D. Dynlacht. 2007. Cep97 and CP110 Suppress a Cilia Assembly Program. *Cell*. 130:678-690.

Tan, D., A.B. Asenjo, V. Mennella, D.J. Sharp, and H. Sosa. 2006. Kinesin-13s form rings around microtubules. *The Journal of Cell Biology*. 175:25.

van Breugel, M., M. Hirono, A. Andreeva, H.-a. Yanagisawa, S. Yamaguchi, Y. Nakazawa, N. Morgner, M. Petrovich, I.-O. Ebong, C.V. Robinson, C.M. Johnson, D. Veprintsev, and B. Zuber. 2011. Structures of SAS-6 Suggest Its Organization in Centrioles. *Science*. 331:1196.

Weaver, B.A.A., A.D. Silk, C. Montagna, P. Verdier-Pinard, and D.W. Cleveland. 2007. Aneuploidy Acts Both Oncogenically and as a Tumor Suppressor. *Cancer Cell*. 11:25-36.

Yamashita, Y.M., A.P. Mahowald, J.R. Perlin, and M.T. Fuller. 2007. Asymmetric Inheritance of Mother Versus Daughter Centrosome in Stem Cell Division. *Science*. 315:518.